

Optical and scintillation properties of Ce^{3+} doped YAlO_3 crystal fibers grown by μ -pulling down technique

M. Alshourbagy*, S. Bigotta, D. Herbert, A. Del Guerra, A. Toncelli, M. Tonelli

Istituto Nazionale di Fisica Nucleare (INFN) and Dipartimento di Fisica dell'Università di Pisa, Largo Pontecorvo 3, 56127 Pisa, Italy

Received 2 August 2006; received in revised form 22 December 2006; accepted 3 January 2007

Communicated by R.S. Feigelson

Available online 4 February 2007

Abstract

We have grown single YAlO_3 crystal fibers using the so-called μ -pulling down technique for scintillation applications. Good quality un-doped and Ce-doped crystal fibers with diameters in the range 0.3–2.5 mm and length up to 150 mm have been grown. A first structural, spectroscopic and scintillation characterization will be presented.

© 2007 Elsevier B.V. All rights reserved.

PACS: 81.05.-t; 81.10.-h; 87.64.Ni; 29.40.Mc

Keywords: A2. Growth from melt; A2. Micro-pulling down; B1. Oxides; B1. Perovskites; B2. Scintillator materials

0. Introduction

At present, various scintillators such as Ti:NaI , Ti:CsI , BaF_2 , etc. are used for many applications in the field of research, medicine and industry. Some new materials, for example CeF_3 , Ce:YAG and others, are being investigated with good results [1]. It is a challenge to find a dense and fast radiation scintillator useful in high energy physics, astrophysics, medicine and other applications. Several studies [2,3] have shown that Ce-doped YAlO_3 (Ce:YAP) is a good candidate as a γ -ray detector. Ce:YAP is an interesting scintillator which exhibits fast scintillation, high light yield and very good mechanical and chemical properties. It has high hardness, it is mechanically and chemically stable and is not soluble in inorganic acids and resistant to alkali. The mechanical properties allow the deposition of very thin layers of reflectors on the surfaces. In comparison to other scintillators, Ce:YAP shows some advantages, in particular: relatively high density, high light yield and short decay time.

Usually, Ce:YAP single crystals are grown by the Czochralski method and then processed (oriented, cut in suitable shape, and polished) to fit the application requirements. The possibility of growing crystals in the shape of fibers with the μ -pulling down (μ -PD) method could open the possibility of cutting production costs of materials because this technique is inherently cheap as for building and running costs. Moreover the samples are directly produced in a shape suitable for applications, thus cutting processing costs as well. The method also permits to have samples in new shapes, not easily obtainable with conventional methods. In this work, we have used the μ -PD method to grow single YAlO_3 (YAP) crystal fibers of high quality and transparency. With this technique we succeeded to incorporate up to 0.7 mol% of cerium into the lattice without constitutional supercooling effects and/or second phase precipitations.

1. Crystal growth

Usually, Ce:YAP single crystals are grown by the Czochralski method in molybdenum or iridium crucibles and in reducing atmosphere. The Ce^{3+} activator ion is 1.18 Å in ionic radius, and has a $4f^1$ electron configuration.

*Corresponding author. Tel.: +39 0502214336; fax: +39 0502214333.

E-mail addresses: malshourbagy@yahoo.com, shourba@df.unipi.it (M. Alshourbagy).

The size of the Ce^{3+} ion and the chemical affinity suggest that the rare earth dopant would preferentially replace the Y^{3+} sites (1.06 Å), rather than the Al site (0.51 Å). But still the ionic radius of Ce^{3+} is 12% larger than that of Y^{3+} , so it is difficult to incorporate a large amount of cerium into the lattice using the Czochralski method without constitutional supercooling effects and second-phase precipitations since the maximum concentration of Ce^{3+} in a single crystal is limited by the segregation coefficient and growing conditions. Another major difficulty encountered during growth by the conventional Czochralski method and subsequent cutting of the crystals is a tendency to crack and twin. This twinning in Ce:YAP crystal can be understood from interchange between the nearly identical a (5.3265 Å) and b (5.1777 Å) lattice parameters [4], which means make the crystal twins easily. Because of the great differences between the thermal expansion coefficients along the three crystalline axes (4.2×10^{-6} , 5.1×10^{-6} and $11.7 \times 10^{-6} \text{ K}^{-1}$ for a , b and c , respectively, in YAP crystals [5]), thermal stresses during crystal cooling should also be responsible for twins and cracks in Ce:YAP crystals.

In this work, the single crystal fibers were grown using the μ -PD technique directly in a shape suitable for scintillation applications. Y_2O_3 , Al_2O_3 and Ce_2O_3 powders of 99.999% purity were used as starting materials. Ce:YAP, powders were mixed in the stoichiometric ratio of $(\text{Y}_{1-x}\text{Ce}_x)\text{AlO}_3$, with $x = 0, 0.002, 0.005$ and 0.007 .

Desired quantities of various compositions were carefully weighed and mixed by grinding in ethanol with an agate mortar and pestle for 15–20 min, and dried at 100°C for 3–5 h. The powder was then cold pressed into 2 mm thick, 10 mm diameter pellets, under 200 MPa pressure. Preliminary sintering was performed by heating these disks in a furnace at 1450°C for 24 h. Mixed powders were loaded into the iridium crucible that was placed on a zirconate pedestal in a vertical high purity and high density Alumina ceramic tube and was inductively heated using RF generator. Compressed alumina and zirconia tubes were used to surround the crucible for thermal insulation. Moreover, a vertical quartz tube was put for better thermal isolation. Our hot zone design is shown in Fig. 1.

A $\langle 001 \rangle$ oriented Ce:YAP parallelepiped of about 2 mm lateral size produced by the Czochralski technique was used as a seed. The crystals were grown at various pulling rates from 0.02 to 0.1 mm/min.

We succeeded in growing un-doped and Ce^{3+} doped YAP single crystal fibers with lengths up to 150 mm and diameters from 0.5 to 2.5 mm. For scintillation applications, we grew Ce^{3+} :YAP shorter fibers (about 10–15 mm in length) but with much larger diameter (≈ 2 –2.5 mm). The aim of this is to compare the scintillation performance of the μ -PD grown crystal fibers with that of a similar size YAP pixel cut and polished from a Cz grown boule that is commercially available and usually used in γ -ray detectors for medical applications.

In order to reach this goal we modified the crucible nozzle to have a 2 mm diameter aperture and we succeeded in growing ≈ 2.5 mm diameter fibers. We observed that the

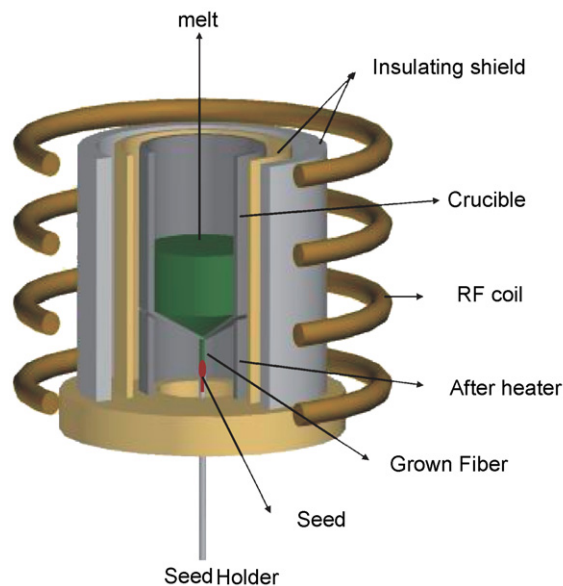


Fig. 1. Schematic diagram for our hot-zone part inside central body of μ -PD growth apparatus.

quality of the fibers was dependent on the pulling rate and better quality fibers were obtained at slower pulling rates. The best fibers were grown at 0.05 mm/min. Photographs of some of the single crystal fibers grown by the μ -PD are shown in Fig. 2. For these Ce^{3+} concentrations, the crystal were almost transparent, crack-free and no garnet phase appeared. No visible inclusions are observed. After growth, as-grown fibers were cut to several test samples with different lengths (5.8, 9.5 and 7.1 mm long for 0.2% Ce:YAP, 0.5% Ce:YAP and 0.7% Ce:YAP, respectively, with diameter varying from 1.5 to 2.5 mm) perpendicular to the growth direction and polished on both surfaces using alumina and diamond powders if necessary. Several samples are used to perform different measurements for characterization.

2. Characterization

2.1. Laue XRD measurement

By means of a Laue chamber we performed X-ray diffraction measurements to check the single crystalline character of the samples and also to identify the crystallographic axes direction. The accelerating voltage was 25 kV, and the tube current was 30 mA with 15 min exposure time. All X-ray experiments were carried out at room temperature. The fibers are single crystal and maintain the seed orientation throughout all their length.

2.2. Spectroscopic measurements

Room temperature absorption measurement was performed on optically polished fibers by means of a spectrophotometer (VARIAN_CARY500). The measurement was performed between 200 and 400 nm with a resolution of 0.1 nm. The emission measurements were performed

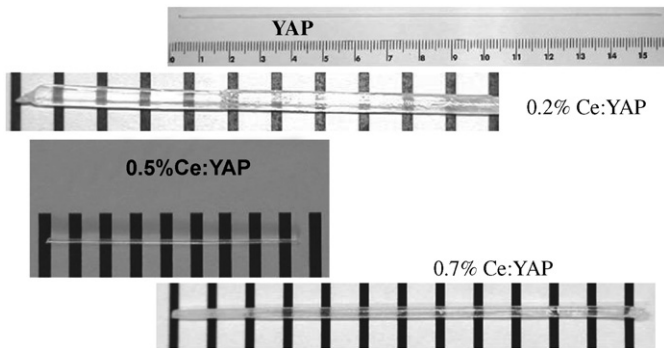


Fig. 2. The obtained un-doped and Ce-doped YAP single crystal fibers.

between 310 and 460 nm by exciting the sample using a 100 W high-pressure mercury-lamp (HBO-100 W) filtered by a 0.1 m Jobin–Yvon monochromator. With this setup we selected the 315 nm emission wavelength from the lamp that was focused on the crystal by means of a 7.5 cm focal length UV-grade silica lens. The emission was mechanically chopped and focused by a 10 cm UV-grade fused silica lens on the input slit of a computer-controlled 0.25 m monochromator and detected by a Hamamatsu R1464 photomultiplier. To avoid the spurious pump scattering, the signal was detected orthogonally to the direction of the exciting beam and processed by a lock-in amplifier. A UV Glan–Thompson polarizer selected the fluorescence polarization parallel (π) and perpendicular (σ) to the c optical axis. The overall resolution of the system was 3 nm. The optical response of the system was normalized for both polarizations by using a deuterium lamp. For the fluorescence lifetime measurements we excited the samples with a laser pulse at 263 nm and a duration of 5 ns full width half maximum (FWHM) by means of a fast phototube with 100 ps rise time and a 500 Gs/s sampling oscilloscope Tektronix TDS520 with a bandwidth of 500 MHz. We acquired the fluorescence decay in the spectral windows selected by using a 0.1 m Jobin–Yvon monochromator.

2.3. Absorption of Ce:YAP: results and discussion

Fig. 3 shows the absorption measurement. The measurement is not polarized because the absorption band of Ce:YAP lies outside the transmission window of our polarizers. As $4f \rightarrow 5d$ transitions are not parity forbidden, they have very high absorption (and emission) cross-sections. This leads to a very high absorption coefficient in the UV absorption region even for low doped samples. This fact, together with the small transversal dimension of our fibers, makes the measurement quite difficult unless the sample is very thin. For this reason very thin optically polished slices of fibers and pixel are prepared for absorption measurements: 0.3 mm thick for 0.2% Ce:YAP, 0.25 mm for 0.5% Ce:YAP, 0.2 mm for 0.7% Ce:YAP and 0.1 mm for Ce:YAP pixel crystal. The comparative results for the Ce^{3+} bands are reported in Fig. 3 together with the

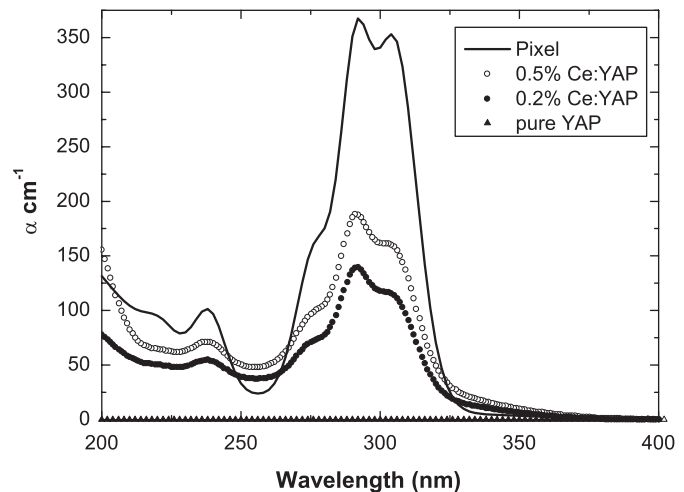


Fig. 3. Ce:YAP absorption spectrum in UV region.

absorption background of the un-doped YAP fiber that shown transparency in the region of interest.

The trivalent cerium ion (Ce^{3+}) with the electronic configuration $4f^1$ has $^2F_{7/2}$ and $^2F_{5/2}$ manifolds separated by about 2250 cm^{-1} due to spin–orbit coupling. The $^2F_{5/2}$ ground manifold is occupied and the $^2F_{7/2}$ manifold is almost empty at room temperature because $kT \approx 200\text{ cm}^{-1}$. The first excited configuration ($5d$) is located at about $40\,000\text{--}50\,000\text{ cm}^{-1}$ [6] and split by the crystal field in 2–5 components. As a result the optical spectra of Ce^{3+} doped YAP crystals consist of f–f transitions in the infrared and f–d transitions in the ultraviolet. For this reason optical absorption bands of Ce^{3+} in 0.2% Ce:YAP, 0.5% Ce:YAP and Ce:YAP pixel are observed due to the electric dipole transitions from $^2F_{5/2}$ ground state to the first $5d^1$ excited state. The spectra show four peaks at 303, 291, 275, and 238 nm. These values are identical and correspond for those in the literatures [7].

According to the spectroscopic data, Weber [6] established the energy level diagram of $4f$ and $5d$ configurations of Ce^{3+} in YAP at 300 K. The four peaks shown in Fig. 3 arise from Ce^{3+} . An additional weak peak at about 220 nm exists in the energy level diagram for Ce^{3+} doped YAP but is not evident in the absorption spectrum of 0.2% Ce:YAP and 0.5% Ce:YAP, instead it is clearly visible in the 0.7% Ce:YAP fiber and Ce:YAP pixel spectra. These five bands are all assigned to the $5d$ levels of Ce^{3+} .

2.4. Fluorescence of Ce:YAP: results and discussion

Fig. 4 shows the polarized emission cross-section spectra, evaluated by means of the so-called $\beta - \tau$ method [8], of the Ce^{3+} in 0.5% Ce:YAP single crystal fiber together with the spectra of the Ce:YAP reference pixel for comparison purposes. These spectra arise from the transitions from the lowest crystal field components of $5d^1$ excited state to the $^2F_{5/2}$ and $^2F_{7/2}$ ground states and present two broad bands largely overlapping with a main peak of $6.61 \times 10^{-18}\text{ cm}^2$ located at 377 nm for the σ polarization and a peak of

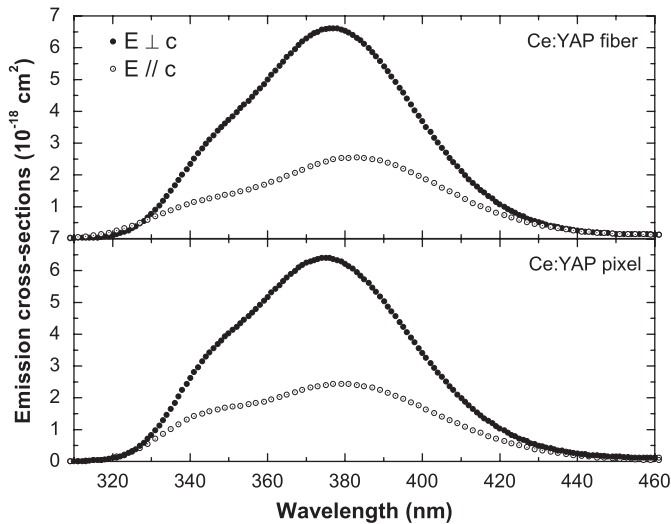


Fig. 4. Polarized room temperature emission cross-sections of the 0.5% Ce:YAP (up) single crystal fiber, obtained from the emission spectra of $5d \rightarrow 4f$, in comparison with Ce:YAP pixel (down).

$2.55 \times 10^{-18} \text{ cm}^2$ at 383 nm for the π polarization. The emission spectra of the reference pixel do not differ from that of the fibers under study. The slight differences observed in the peak positions and in the line shape, may be ascribed to artifacts due to different re-absorption processes inside the two samples. Indeed, due to the very high line strength of the transition it is possible that some photons in the short wavelength part of the emission spectrum are re-absorbed before escaping the crystal. Since this probability depends on the doping concentration and on the geometry of the sample, different specimen may exhibit small differences in their spectra.

For the lifetime measurements the excitation density was changed by varying the pump pulse energy and the focusing conditions. We did not find any relevant difference in the temporal shape of the decays by varying the excitation densities in the exploitable range up to 2 J/cm^2 . For a determination of the lifetime, a single exponential fit was performed but disregarding the first 15 ns after the rise of the fluorescence emission. In this way, we considered the evolution of the fluorescence emission in the absence of the excitation pulse. We performed the decay time measurement on our three fibers and on a Ce:YAP crystal (pixel) grown by Czochralski method for comparison. Experimental lifetime values have been fitted to a unique exponential profile and the decay time was found to be 22 ns with an excellent agreement with literatures [9].

3. Scintillation performance of Ce^{3+} doped YAP fibers

The scintillation light yields were measured under γ -ray excitation (^{22}Na). The measurement setup was a simple γ -ray spectroscopy arrangement based upon a photomultiplier tube and multichannel analyzer.

The photomultiplier used was the 12-stage XP2020 from Photonis, which is often employed for quantitative studies

of scintillator light yield. The XP2020 has a gain of 3×10^7 at 2 kV. Measurements were made at a HV of 2150 V, an amplifier gain of 25 and shaping time constant of 500 ns unless otherwise stated. The PMT output signal is amplified and shaped by an Ortec 570 NIM module. This signal is then sent to a Tukan8k ADC and MCA PCI card for acquisition and display. The various scintillators used in this test, including the fiber pieces, were first wrapped in PTFE (teflon) tape on all sides, except the surface coupled to the PMT. The tape increases the light yield by providing a diffuse reflection of any light that escapes the crystal, such that it might reach the PMT. The scintillators were then coupled to the PMT entrance window with optical coupling grease of refractive index 1.46. We performed the measurement on our fibers and in comparison with standard crystal (pixel) grown by Czochralski method.

The photoelectron yield is defined as the number of photoelectrons (N_{pe}) created at the photocathode of the PMT. The relationship between this number and the original number of photons per MeV (Ψ) is

$$N_{pe} = \Psi \cdot \varepsilon_{QE} \cdot E_{\gamma} \cdot \eta, \quad (1)$$

where E_{γ} is the γ -ray energy in MeV, η is the light collection efficiency and ε_{QE} is the average quantum efficiency. In this paper, we attempt to estimate the photoelectron yield of the YAP fiber samples in two ways:

- By making a comparison with a calibrated scintillator.
- Using the single photoelectron electron peak of the XP2020 (Bertolaccini method [10]).

3.1. Results of comparative light yield

The spectra in Fig. 5 show the energy loss of gamma rays in a commercially produced $2 \times 2 \times 10 \text{ mm}^3$ Ce:YAP crystal, a 0.2% Ce:YAP fiber and a 0.5% Ce:YAP single crystal fibers. We repeated the measurements for all sample crystals under investigation in the same measurement conditions, several times each. Table 1 shows a summary of the results, including the relative light outputs and the energy resolution at 511 keV (when the measurement is possible). Representative spectra for each of the fiber samples and the YAP pixel are shown in Fig. 5.

From this Table and Fig. 5 it can be seen that the two fiber samples have virtually the same light output. This is seen from the position of the Compton edge. However, the obvious observation is that the 0.5% sample has a much better energy resolution than the 0.2% sample because it has a clear photopeak visible. The fiber with 0.2% Ce doping has no visible photopeak, which is strange as, normally, the resolution depends upon the photon statistics which are virtually the same as for the 0.5% sample. Therefore, the degradation of the energy resolution must come from another source. This could be due to non-uniform doping of the cerium, very high absorption or

non-uniform light collection from surface or crystal imperfections, or fluorescence killer centers. Moreover, the fiber samples have $\sim 40\%$ light output with respect to the Ce:YAP pixel.

3.2. Results of absolute photoelectron yield

Two calibration methods were employed to estimate the absolute light yield; Firstly using a calibrated reference crystal and secondly via an absolute calibration of the photomultiplier using the Bertolaccini method [10].

3.2.1. Crystal calibration

A thin disc of BGO was used ($\varnothing 10\text{ mm} \times 1\text{ mm}$) to provide an estimate of the N_{pe} . BGO was chosen as it has a well defined light yield (Ψ) and has a high enough density and Z to stop a reasonable number of gammas and have a good photopeak. The flat surfaces were fine ground to reduce the contribution of the light trapped due to total internal reflection. This is particularly important for BGO as it has a high refractive index ($n = 2.15$).

As with the other tests, multiple acquisitions were made to account for coupling differences, and average values of the 511 keV photopeak position, Compton edge and energy resolution recorded. Results are again shown in Table 1. Since BGO is our standard we will calculate the number of N_{pe} that we would expect *theoretically* for a 511 keV deposit

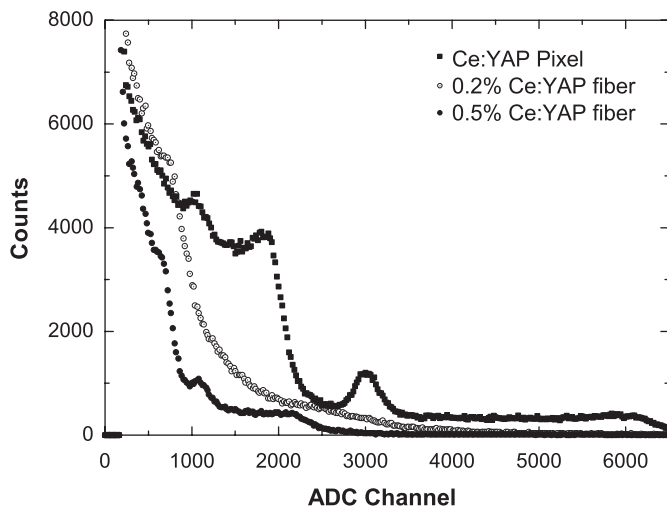


Fig. 5. Spectrum of 0.2% Ce:YAP and 0.5% Ce:YAP in comparison with commercially produced $2 \times 2 \times 10\text{ mm}^3$ Ce:YAP crystal.

Table 1

Summary of the results from the measurements made with different scintillators (RLO = relative light output)

Scintillator	Compton edge (chn)	Photopeak (chn)	FWHM (@511 keV)	RLO (%)	N_{pe} (scint. cal. method)	N_{pe} (PMT cal. method)
Ce:YAP pixel	1875 ± 18	3022 ± 13	10.8 ± 0.2	100	1314 ± 228	833 ± 16
0.5% Ce:YAP	712 ± 34	1191 ± 62	15.9 ± 1.4	39	518 ± 149	328 ± 18
0.2% Ce:YAP ^a	743 ± 15	–	–	41	549 ± 99	347 ± 18
BGO	880 ± 10	1391 ± 59	14.8 ± 0.7	46	605 ± 109	383 ± 18

^aPhotopeak values extrapolated from Compton edge position.

using Eq. (1). We assume a light yield of 8200 ph/MeV and the average quantum efficiency of the XP2020 over the emission wavelengths of BGO is 15%. The LCE (η in Eq. (1) is more difficult to estimate. There are two articles in the literature that make reference to the η of BGO of very similar geometry; One article [11] states a η of 71% for a geometry of $10 \times 10 \times 2\text{ mm}^3$ whilst the other [12] cites about 95% for a geometry of $\varnothing 9\text{ mm} \times 1\text{ mm}$. We choose to use 95% as the geometry is nearly identical to ours and the figure is based upon measured data as opposed to the former, which is based upon extrapolation from simulated data. Employing Eq. (1) and the figures mentioned above, we arrive at a figure of 600 ± 90 photoelectrons. Using the measured average 511 keV photopeak position of 1391 ± 59 chn, this leads to a calibration of 2.3 ± 0.4 channels per photoelectron. Applying this to photopeak positions of the YAP fibers this gives 518 ± 149 and 549 ± 99 photoelectrons for the 0.5% and 0.2% Ce samples, respectively.

3.2.2. PMT calibration

We observed the single photoelectron peak of the XP2020 at channel 145 ± 2.3 for an amplifier gain of 1000. Our measurements were made at a gain of 25, giving a calibration factor of 3.63 ± 0.07 channels per photoelectron at the measurement settings used. Applying this to the photopeak positions of the YAP fibers this gives 328 ± 18 and 347 ± 18 photoelectrons for the 0.5% and 0.2% Ce samples, respectively.

The photoelectron numbers using this calibration method are also summarized in Table 1.

3.3. Conclusion

For the first time we succeeded to grow Ce-doped YAP single crystal fibers by μ -PD method with different lengths and diameters. Absorption and emission spectra are in good agreement with literatures. The light yields from the fibers in comparison to a similar sized commercial YAP pixel were around 40% but similar to BGO crystal. Moreover the two tested samples were found to have very similar light yields, differing by 5% even though they had different doping levels. Strangely, despite the similar light yield, the 0.2% cerium sample did not display a visible photopeak whilst the 0.5% sample did, thus implying poor energy resolution. These results are encouraging if one takes into account that the crystal features of our fibers are not completely optimized. In particular, work is in progress in order to

optimize the quality of the crystal fibers, the light collection efficiency, their size, and the Ce doping level.

Acknowledgment

The authors wish to thank Mrs. Ilaria Grassini for the preparation of the samples and Dr. Daniela Parisi for X-ray diffraction measurement and useful discussion.

References

- [1] S. Andersen, et al., Nucl. Instrum and Methods A 332 (1993) 373.
- [2] J.A. Mares, M. Nikl, K. Blazek, Phys. Status Solidi A 127 (1991) K605.
- [3] J.A. Mares, et al., Mater. Chem. Phys. 32 (1992) 342.
- [4] G. Neuroth, F. Wallrafen, J. Crystal Growth 435 (1999) 198–199.
- [5] G.J. Zhao, X.H. Zeng, S.M. Zhou, J. Xu, Y.L. Tian, W.X. Huang, Phys. Status Solidi (a) 199 (2) (2003) 186–191.
- [6] M.J. Weber, J. Appl. Phys. 44 (1973) 3205.
- [7] S. Kammoun, M. Kamoun, Phys. Status Solidi (b) 229 (3) (2002) 1321–1327.
- [8] B. Aull, H. Jenssen, IEEE J. Quantum Electron 18 (1982) 595.
- [9] M. Nikl, Phys. Status Solidi (a) 178 (2002) 595.
- [10] M. Bertolaccini, S. Cova, C. Bussolatti, A technique for absolute measurement of the effective photoelectron per keV yield in scintillation counters, in: Proceedings of the Nuclear Electronics Symposium, Versailles, France, 1968.
- [11] E. Sysoeva, V. Tarasov, O. Zelenskaya, Nucl. Instrum Methods A 486 (2002) 67–73.
- [12] M. Moszynski, M. Kapusta, M. Mayhugh, D. Wolski, S.O. Flyckt, IEEE Trans. Nucl. Sci. NS-44 (1997) 1052–1061.